Coupling high strain rate experiments with numerical simulation for material model calibration: application to lightweight armor

H. Abdulhamid[1], J. Mespoulet[1], P. Deconinck[1] and P. Héreil[1]
[1]*Thiot Ingénierie, 830 route Nationale, 46130 Puybrun, France*
abdulhamid@thiot-ingenierie.com

Abstract. This paper presents a comprehensive mechanical study of a lightweight armor structure composed of two different kind of materials: a ceramic tile and a UHMWPE (Ultra High Molecular Weight Polyethylene) layer. The aim of this study is to provide reliable experimental data for building and validation of the whole structure under impact loading. For each material, a building block approach was used to characterize from the specimen to the structure; and a material model is fed at each step. Concerning the ceramic material, Hugoniot and spall parameters were at first identified using plate impact tests. Dynamic compression tests on Split-Hopkinson Pressure Bars (SHPB) were performed on confined specimens to analyze the effects of pressure on the damaged strength. Ballistic impacts on metal-backed ceramic tiles were performed to measure its strength in a typical shielding application. Experimental data was used to calibrate a Johnson-Holmquist (JH-2) model. For the UHMWPE, in-plane tension, and out-of-plane compression and shear were performed. This material exhibited very low shear modulus and peeling strength. Ballistic impacts have been performed on larger specimens. Based on these results, an elasto-orthotropic law with damage model was calibrated. At the end, a final validation test was performed on the armor made with the two characterized materials.

1 INTRODUCTION

Standard soldier lightweight armor (
Figure **1**) consists of a ceramic tile (2), a UHMWPE plate (3) and a polymeric foam (4). The impact fragments both the projectile (1) and the ceramic tile. The role of the UHMWPE is to decelerate and catch most of the generated fragments. The polymeric foam helps not only catching the last fragments but also reducing the impulsion transmitted to the soldier's chest.

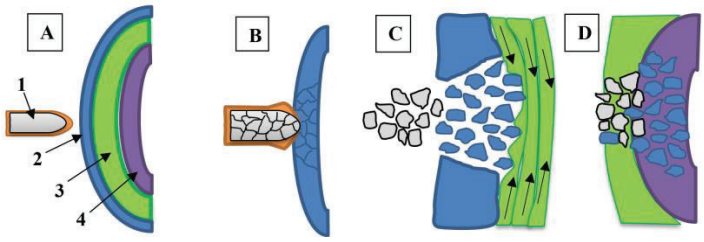

Figure 1. Soldier lightweight armor constitution

The methodology presented in this paper combines multiple experimental tests and finite element simulations in order to study the dynamic behavior of both a ceramic and UHMWPE materials. This combination helps reducing research time and cost. On one hand, experimental tests help identifying the most prominent phenomena to consider and provide data for model parameters. On the other hand, numerical simulations improve the comprehension of phenomena mechanisms especially for dynamic events that are too brief and complicated to be observed experimentally. Therefore, an iterative approach between tests and numerical simulations with a Building Block Approach (BBA - Figure 2) was conducted: studying material behavior from simple coupons to configurations with complex assemblies.

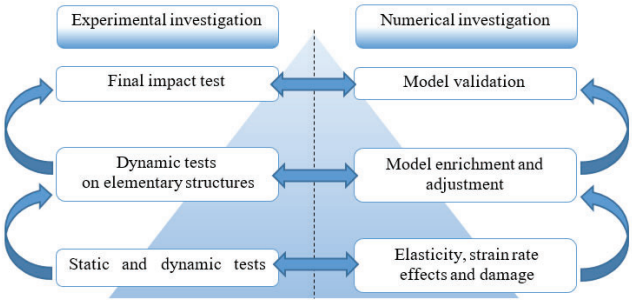

https://doi.org/10.52202/078352-0019

Figure 2. The Building Block Approach

The BBA consists in analyzing the material response from mesoscopic to structure scales. The material models in LS-DYNA were enriched throughout the tests with parameters characterizing the linear elastic response, strain rate effects and damage evolution.

For ballistic armors, and due to their weakness in tension, ceramic tiles are backed by a ductile plate to provide tensile strength to the armor configuration. In such configuration, the ceramic tiles are mainly loaded in compression and fragment the projectile while the backing prevents any penetration of the debris [1]. The design through numerical simulation of a solution to withstand a given threat remains challenging. One of the reasons is related to the difficulty to fully characterize the behavior of ceramics [2]. They show brittle failure but they can withstand important compressive load and undergo large deformation once damaged. This compressive strength depends on the confinement and is particularly important to the resistance to impact of the shield [3]. Therefore, it is important not only to measure the intact response of the ceramic but also to characterize the material in its damaged state under different confinement levels. Direct measurement of the damaged strength of brittle material is difficult to perform and indirect measurement are usually realized instead [4] [5]. A Johnson-Holmquist damage law (JH-2) [6] is calibrated. The experimental study consists in plate impact, dynamic compression of confined specimen on SHPB and impact tests. Results of numerical simulations from LS-DYNA are compared with experimental data. The purposes of the approach are both to evaluate the ability of the JH-2 to reproduce the tests and to provide additional information for the analysis of experimental data.

The use of polymer-based composite like ultra-high molecular weight polyethylene (UHMWPE) has become popular in lightweight armors. Such materials can exhibit diverse failure modes depending on the characteristics of the threats. Therefore, it is convenient to use numerical tool for the analysis and optimization of such type of armor. Many studies have been conducted on UHMWPE composite material dynamic response. For example, [7] investigated in-plane deformation behavior and [8] shock propagation in-fiber direction. Out-of-plane compressive response has been studied by [9] in static and [10] under shock loading. Furthermore, a comprehensive literature is available regarding, the ballistic response of this material [11] [12]. [12] used a numerical model combining orthotropic behavior and EOS for the simulation of ballistic response on UHMWPE plate. In this work, the mechanical response and failure mode are investigated under three types of dynamic solicitation: in-plane tension, out-of-plane compression, and out-of-plane shear. Then, impact tests are performed with spherical projectile. Experimental data is then used as input of an orthotropic material law coupled with fiber damage.

The paper is divided into three parts, the first details the characterization tests with corresponding model and the second deals with the ballistic tests and simulation. The last part is dedicated to the final validation test. Some results had to be normalized to comply with confidentiality obligations of the study.

2 MATERIAL CHARACTERIZATION

2.1 Ceramic material

The aim of this part is to calibrate a Johnson-Holmquist damage model (JH-2) that is commonly available in commercial finite element softwares. Inside LS-DYNA, the JH-2 is implemented as *MAT_110. It has been developed to model the failure of brittle materials like glass or ceramics under high strain rate. The JH-2 model consists of two main blocks. First, a linear elastic law defined by a material Equation Of State (EOS) and a shear modulus. Second, a damage evolution law which describes the failure strength of the material. The EOS is given by Equation (1).

$$P = K_1\mu + K_2\mu^2 + K_3\mu^3 + \Delta P_{n-1} \tag{1}$$

where μ is the material volumetric strain; P is the mean stress assimilated to the material pressure; K_1, K_2 and K_3 are the Hugoniot parameters which are determined from plate impact tests and ΔP_{n-1} is computed by Ls-Dyna from the amount of accumulated damage. One of the main characteristics of the JH-2 model is the pressure dependence of the material strength (

Figure 3). The material strength during damage evolution under compressive loading is defined by two curves $\sigma_i(P, \dot{\epsilon})$ describing the intact strength and $\sigma_f(P, \dot{\epsilon})$ the fractured strength and a damage variable D. The material strength is between those two curves during damage evolution and then follows σ_f once it is fully damaged.

$$\sigma = \sigma_i - D\,(\sigma_i - \sigma_f) \tag{2}$$

https://doi.org/10.52202/078352-0019

Where :

$$\sigma_i = \sigma_{HEL}\, A \left(\frac{P+T}{P_{HEL}}\right)^N (1 + \mathrm{C} \ln \dot{\epsilon}\,) \tag{3}$$

$$\sigma_f = \sigma_{HEL}\, B \left(\frac{P}{P_{HEL}}\right)^M (1 + \mathrm{C} \ln \dot{\epsilon}\,) \tag{4}$$

$$\Delta D = \frac{\Delta \epsilon_P}{D_1 \left(\frac{P+T}{P_{HEL}}\right)^{D_2}} \tag{5}$$

A, B, M, N, T, D1 and D2 are the material parameters. σ_{HEL} and P_{HEL} are calculated from an impact plate test data in which the HEL is reached (TI1131). Then, the value of A and N are computed so that σ_i is equal to σ_{HEL} at $P = P_{HEL}$. The damage parameters B, M, D_1 and D_2 cannot be directly measured from experiments but need to be calibrated to reproduce numerically a set of failure tests.

The ceramic material is available in blocs of 100 x 100 mm² square area with 5 or 20 mm thickness. It has then been machined to manufacture the specimens used in this study.

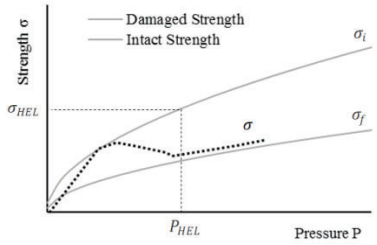

Figure 3. Description of Johnson-Holmquist damage model

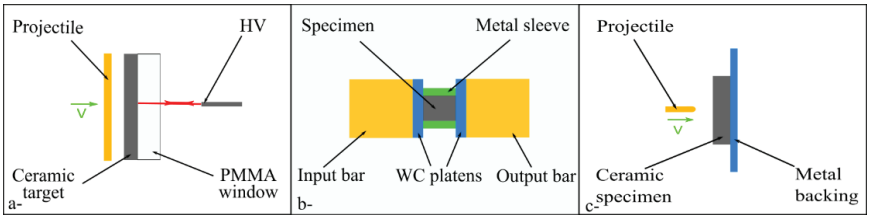

Figure 4. Schematics of experiments, a- plate impact, b- dynamic compression of confined specimens on SHPB, c-ballistic

2.1.1 Plate impact tests

Figure 4a shows the configuration of the plate impact tests. Copper disk projectiles are used for the experiment and PMMA windows are glued at the back of ceramic targets. All dimensions are defined so that the release stress waves do not interfere with the longitudinal stress during the period of observation. A Photonic Doppler Velocimeter (PDV) is used to monitor the normal velocity at the interface between target the PMMA. Figure 5 compares the velocity profiles recorded for three tests corresponding to different impact velocities and/or projectile thicknesses. HEL (Hugoniot Elastic Limit) state is reached only for test T1131 and the inelastic response is characterized by the ramping behavior the velocity profile. Taking into account the PMMA impedance, the HEL parameter is computed from experiment T1131 and the evolution of spall strength with impact velocity is obtained from all three curves.

Plate impact tests are simulated using a 2D-axisymmetric model. Element size of 0.05 mm are used to reproduce the shock shape of the velocity signal shown in Figure 5. Figure 6 shows the propagation of the shock wave, along y direction, inside the specimen for test T1131. The comparison of velocity profile shows good agreement with the tests. The model is able to reproduce the maximum velocity at the interface. This result shows that the elastic properties and the EOS have been well identified. Moreover, the HEL velocity for test T1131 is well predicted even though the curvature is not similar.

https://doi.org/10.52202/078352-0019

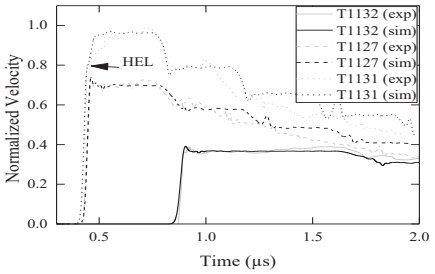

Figure 5. Velocity profiles

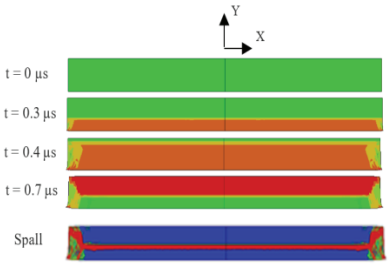

Figure 6. Simulation of plate impact tests

2.1.2 Dynamic compression of confined specimens

The configuration for SHPB tests is presented in
Figure **4**b. Cylindrical ceramic specimens are shrink-fitted inside metal sleeves of 1.5 mm thickness. Three different sleeve materials (copper, aluminum and steel) have been selected to adjust the level of confinement. Also, a copper pulse-shaper is placed between the striker and the input bars to generate an incident pulse with a ramp history.

Figure 7a and b show typical SHPB pulse signals for two tests with copper sleeve. All parameters of the tests are identical apart from the initial velocity. For comp-A test, transmitted pulse has a similar shape to incident pulse. The specimen has not been significantly damaged and only some small cracks are observed. However, for specimen comp-B, there is an abrupt discontinuity in the transmitted pulse. The ceramic has been recovered in a state of powder and the sleeve has collapsed due to buckling. Since the transmitted pulse is proportional to the load passing through the specimen, it can be noted that failure of comp-B occurs at around 60% of the maximum load passing through specimen comp-A. This result is counter-intuitive but quite repetitive and has been observed for all three types of sleeve. Furthermore, a gain in the failure load is observed as the confinement pressure increases (Figure 7c).

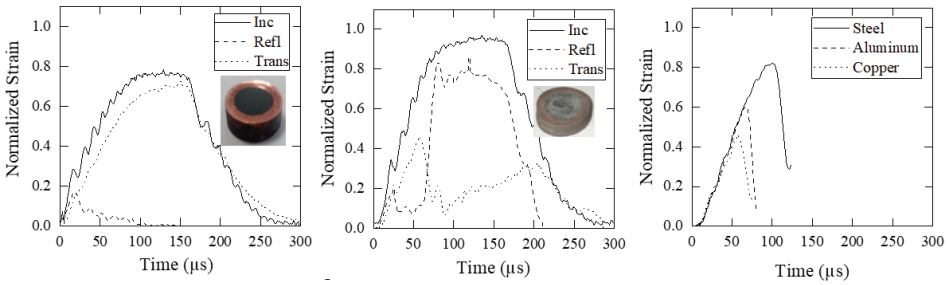

Figure 7. Strain pulses obtained from SHPB experiments, (a-) specimen comp-A, (b-) specimen comp-B, (c-) effects of confinement

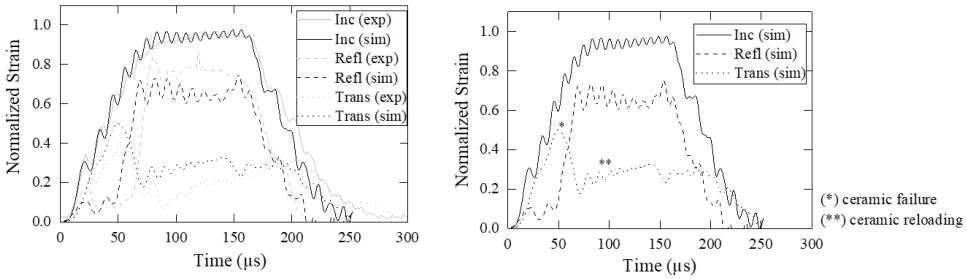

Figure 8. Comparison of SHPB pulses signal shape of specimen comp-B from numerical simulation with experimental data

The simulation of SHPB tests aims to provide additional information for the analysis of the tests results. They are simulated with 2D axisymmetric model. Apart from the ceramic and the sleeve, all the parts of the model are defined with their elastic material property. With the JH-2 parameter set initially used for the plate impact test, the model is not able to reproduce the results of comp-B test. The specimen is not damaged and the pulse signal shapes are similar to that of comp-A specimen. In order to reproduce

https://doi.org/10.52202/078352-0019

the pulse signals of comp-B specimen, the values of A and N needs to be calibrated reducing the intact strength of the ceramic. Figure 8 shows the pulse signals from the simulation. The incident pulse is well reproduced. However, reflected and transmitted signals do not match perfectly the experiment even though similar behaviors are observed. First, a linear response of the ceramic is observed until failure which is characterized by the abrupt drop in the transmitted signal. Then, the damaged ceramic is reloaded and important deformation is observed due to the buckling of the sleeve. In this test, the ceramic failed at a stress far below its HEL, therefore this experiment is complementary to the plate impact test.

2.2 UHMWPE material

The material is available as a laminate panel of UHMWPE unidirectional fibers. It is the strongest fiber available in terms of strength to weight ratio [13] and is obtained from multiple stack 0°/90° plies impregnated with thermoplastic matrix. All the tests conducted have been realized from the same batch of material.

2.2.1 Dynamic tension

Tensile tests are conducted on a 200 tons dynamic press. Tensile load is measured with a piezoelectric sensor. Displacement is measured with a laser sensor. Specimen shape is similar to conventional tensile tests with a rectangle working area of 10 x 6 mm and is loaded at 40 s^{-1} along the fiber direction (0° and 90°). Any attempts to load the 45° direction fails due to a very low in-plane shearing strength. An average 10 % increase of the strength is observed during dynamic tests compared to quasi-static data.

2.2.2 SHPB compression

Compression tests are conducted on Hopkinson bars. Compressive loading is applied in the out-of-plane (o-o-p) direction of the specimen. Eight tests are realized with three different mean strain rates: 3000, 4500 and 5600 s^{-1}. The compressive stress versus strain of the material exhibits a linear response until failure. A 20% increase of the failure strength is observed at high strain rate (Figure 9). The compression failure mode of this material is not conventional as failure is triggered by ply slipping near the edges as shown in Figure 10. Due to very low in-plane shear strength, ply cannot sustain the shear stress induced by the compressive load. Slipping is initiated near the edges since the material is less confined in this area. Similar behavior has been reported under quasi-static loading [9].

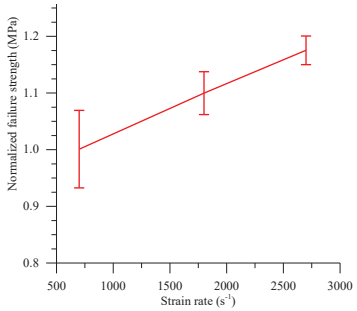

Figure 9. Strain rate effect on failure strength

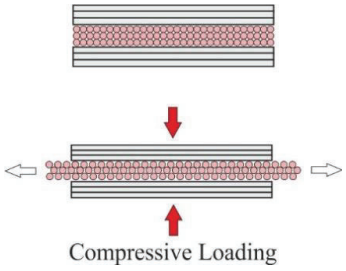

Figure 10. Failure mode under compression

2.2.3 Dynamic shear

A mean o-o-p shear response is measured with the configuration presented in Figure 11a. A cylindrical specimen is clamped on its edge and impacted by a cylindrical projectile. The diameter of the impactor is chosen to be slightly smaller than the inner diameter of the specimen clamp to generate shear stress in the area in between (Figure 11b). A load cell records the loading transmitted through the shearing of the specimen. The specimen back face velocity is measured with a PDV head and is integrated to compute the displacement δ of the specimen. The shearing angle and the shear stress are computed as:

$$\alpha = Arctan\left(\frac{\delta}{l}\right) ; \tau_{mean} = \frac{F}{\pi D e}$$

https://doi.org/10.52202/078352-0019

where D and e are the inner diameter of the clamping tool and the thickness and F the force.

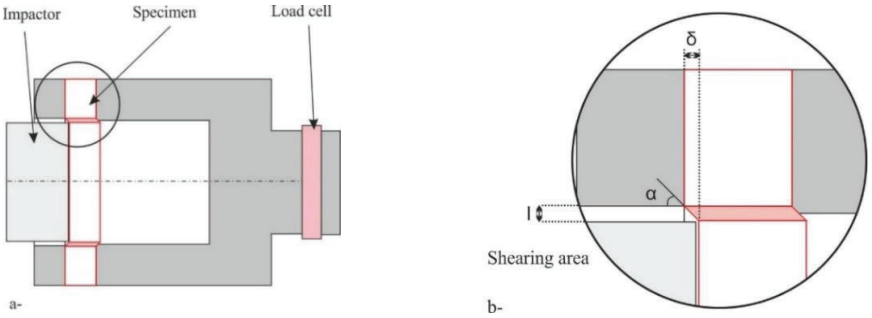

Figure 11. Dynamic shear tests configuration

Four tests are realized with different specimen thicknesses. Figure 12 shows the normalized shear stress versus shear angle curves. The strain rate ranges between 4000 and 5500 s^{-1}. The material response is quite similar for all specimen thicknesses: it confirms that the flexure contribution of the loading is negligible. The response is bilinear: a moderate slope up to 0.4 shear angle then followed by a steeper slope. The first loading phase corresponds to a pure shearing. As the displacement increases, some load is transferred as tension into the fibers which explains the increase in the slope rate.

The identification of the shear modulus G13 and G23 is realized through numerical simulations. The FE model is designed to replicate all the specificity of the testing condition (impactor, boundary condition, load cell …). A linear orthotropic model is used. The value of G13 and G23 is calibrated until the curves fit the experimental data (Figure 12). Figure 13 shows the localization of the shearing in the specimen. Identifying the shear modulus G13 and G23 can only be conducted through this method since experimental force represents a homogenized shear response along the circumference of the specimen.

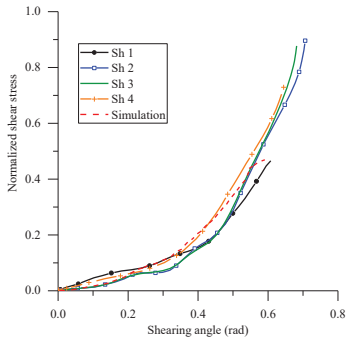

Figure 12. Normalized mean shear stress vs shearing angle

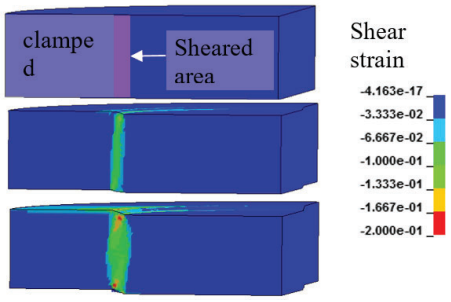

Figure 13. Simulation of the dynamic shear test

3 INTERMEDIATE IMPACT TESTS

3.1 Impact response of ceramic material

Two impact tests (bal-A and bal-B) have been performed with the configuration illustrated in Figure **4**c. In both cases, a steel rod projectile of 35 mm long and 10 mm diameter impacts the target. It consists of a ceramic tile with a surface area of 100 x 100 mm^2 which is tied to an aluminum plate of 150 x 150 x 6 mm^3 dimensions at its back. Two different tile thicknesses have been tested in order to study the perforation resistance of the material: 5 mm for test bal-A and 20 mm for test bal-B. The projectile is launched with a light gas gun and the impact velocity is measured with an optical barriers system. For both tests, the impact velocity is 945 ± 10 m/s and the obliquity of the projectile, measured with an X-ray flash photography is below 2°. For specimen bal-A, a high speed camera is used to record the back side of the target, two images recorded respectively at 10 µs and 280 µs after impact are shown in Figure 14a and b. First, there is a small indentation behind the aluminum backing and later ejected

https://doi.org/10.52202/078352-0019

debris form a typical bi-conical shape. The ejection speed estimated from the camera is 750 ±10 m/s. After impact, the entire ceramic tile has been disintegrated and a hole of 18 mm diameter is present in the backing (Figure 14c). Specimen bal-B is not perforated. Increasing the ceramic thickness has stopped the projectile. The aluminum backing is severely indented and the ceramic tile is fragmented.

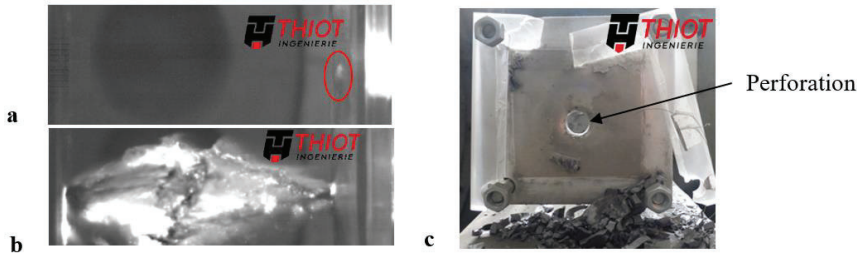

Figure 14. (a-) and (b-) Images of the side of specimen bal-A taken with high speed camera respectively at 10 µs and 280 µs after impact and (c-) perforation of the aluminum backing after the test

One of the goal of this simulation is to reproduce the velocity profile recorded with the PDV head at the backside of the backing of specimen bal-B in order to be able to analyze it. This signal is a result of both the wave propagation inside the target and its structural response. Different modelling approaches have been tested by using solid elements, SPH and hybrid Lagrange/SPH elements. Pure solid elements model gives quite good results as long as the material does not undergo large deformation (until 5-8 µs after impact). The use of SPH elements enables to go further in the calculation but the interaction of SPH elements with different material properties is quite complex. Typically, using the SPH elements interaction to represent the projectile/ceramic and ceramic/backing contacts results in inappropriate reproduction of the wave propagation inside each material and an improper contact separation when required. Also, hybrid elements generate some undesired waves when the solid elements are converted to SPH elements. A compromise is found by modelling the projectile with SPH elements and the remaining parts with solid elements. Benefitting from the symmetry of the problem, only one half of it is modelled as shown in Figure 15.

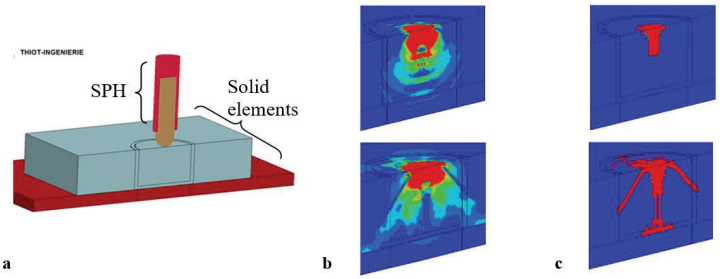

Figure 15. (a) Ballistic impact model, (b) pressure field, (c) damage behind the shock wave

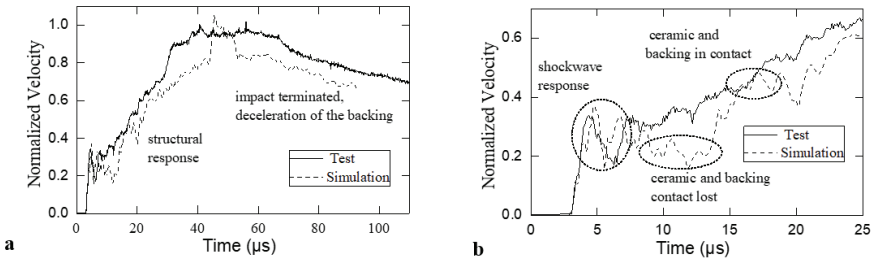

Figure 16. Comparison of the velocity profile at the backside of the backing for bal-B specimen

The projectile is modelled as elastoplastic with a failure strain of 10%. An element erosion criterion at 100% of deformation is added to the ceramic. When the projectile hits the target, two spherical shock waves are generated; one in the target and another inside the ceramic tile. As the ceramic wave propagates, it starts to partially damage the area just below the impact point. Then, the projectile

https://doi.org/10.52202/078352-0019

disintegrates and simultaneously a network of cracks propagates inside the ceramic. Figure 16a and b compare the velocity profile obtained from the simulation with the experimental data. Figure 16a shows that the global response of the armor system is well reproduced. After the initial oscillations, a steady increase of the velocity is observed. This later characterizes the structural response of the target. As the projectile is disintegrating, the force applied to the ceramic decreases resulting in the plateau velocity observed from 35 to 70 µs. Finally, the decrease of the velocity is mainly governed by the aluminum backing. Zooming at the beginning of the curve, (Figure 16b), the initial oscillation is a result of the shock wave interaction with the backing. The gap from 9 to15 µs is due to a loss of contact at the ceramic/backing interface which may not happen in the experiment since the glue is not modelled.

3.2 Impact response of UHMWPE material

The study of the UHMWPE material is completed with impact tests. The test configuration is presented in Figure 17. A 25 mm steel sphere is launched with a gas gun. The target, a disk of 150 mm of diameter is clamped around its edge. The backface velocity is monitored with a PDV system and is observed with a high-speed camera through a mirror. Two tests are performed with different target thickness to obtain non-perforated TI1406 (Figure 19) and perforated TI1408 cases (Figure 20).

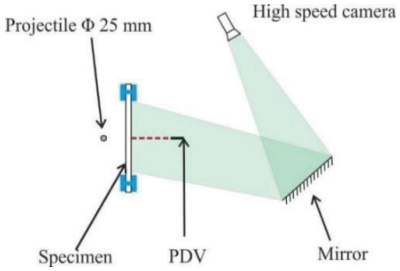

Figure 17. Ballistic tests configuration

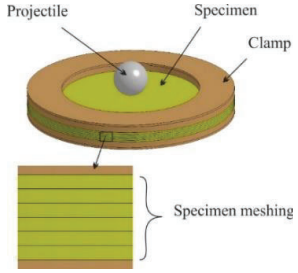

Figure 18. FE model for ballistic impact

For TI1406 specimen, one third of the plies from the front side are perforated. The projectile is recovered in between plies after impact. Important ply interface delamination is observed on the perforated plies. However, the non- perforated group of plies has been compressed and densified. Around the impact point, the nature of the polymer has also changed as if it has been heated close to its melting point. The camera images show that the target undergoes an important back face deformation. Post-mortem analysis of the recovered target shows that non-failed plies undergo large slipping which explains the non-round shape of the specimen edge after the test. For TI1408 test, a thinner target is impacted at a higher projectile velocity. The target is completely perforated. Its deformation is not as important as TI1406 however similar signs of temperature increase is found around failed plies.

Considering all the information gathered throughout the characterization tests and the ballistic impact, a FE model of the ballistic test is realized in LS-DYNA (Figure 18). The target is modelled in 3D at a pseudo-meso scale. Since representing each couple of 0°/90° plies by one element through the thickness would result in very large model, it has been decided to represent a set of 0°/90° by one element. Regarding the material law, initially, the orthotropic model developed for dynamic shear calibration is used with the tensile failure strength measured during material characterization. This version results in the perforation of both ballistic cases with a little decrease in the projectile speed. The target does not have time to deform before it is perforated. To improve the simulation results, a damage model is added to the material model using MAT221 in LS-DYNA. The parameter for damage evolution is set to reproduce the results of TI1408. This modification is motivated to account for the softening due to temperature increase before ply failure. The comparison of obtained back face velocity and projectile residual velocity with the experimental data is shown in Figure 20. The cinematics of the deformation and perforation are also coherent with the test. The target is perforated before important ply slipping. This model is then used to simulate TI1406 test and results in a partially perforated target like in the test. Furthermore, important plies slipping has occurred along the 0° and 90° as in the experiment.

4 FINAL VALIDATION

A final validation has been achieved on HERMES two-stage light-gas gun. The main goal of this test was to evaluate the prediction capabilities of the numerical developed throughout characterization and

https://doi.org/10.52202/078352-0019

intermediate impact tests for both materials. This section only presents the impact test results as the simulations are still under progress. The target is composed of a 5mm thick ceramic tile in front of a 11mm thick UHMWPE panel. The boundary conditions are free for both the ceramic and the composite material, for representativeness of the test compare to a bullet-proof vest. The projectile is a 9.75g 7.62 lead core with copper sleeve bullet launched at 795m.s^{-1}. Two high-speed phantom cameras are used to monitor the impact: a V1840 at three quarter front view and a V2012 on one side. The images are presented in Figure 21. The post-mortem recovery of the composite panel shows that it helped catching the bullet and ceramic fragments. The ceramic tile and the UHMWPE panel thicknesses are sufficient to catch the bullet without any perforation of the composite material. These images will help evaluating the prediction capabilities of the developed numerical models.

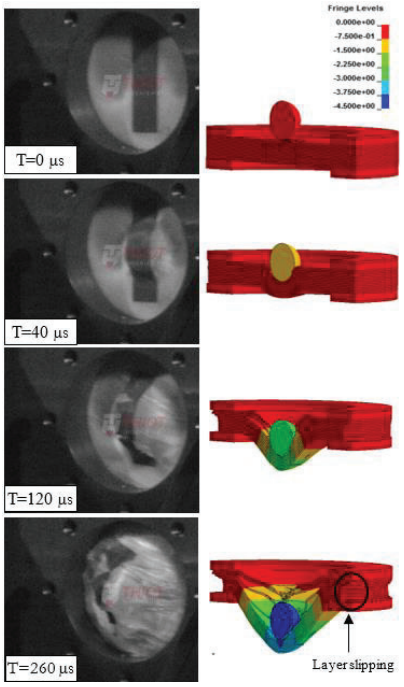

Figure 19. Non-perforated impact test (TI1406), simulation shows the z-displacement

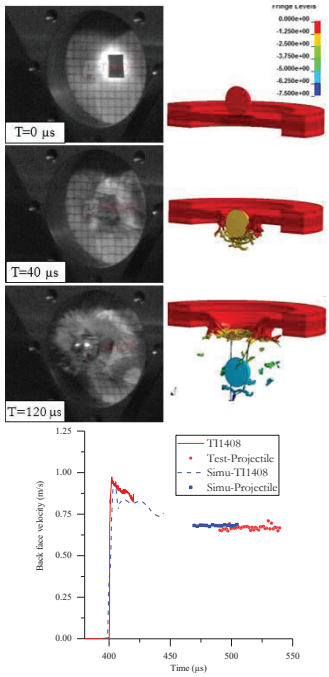

Figure 20. Perforated impact test (TI1408), simulation shows the z-displacement

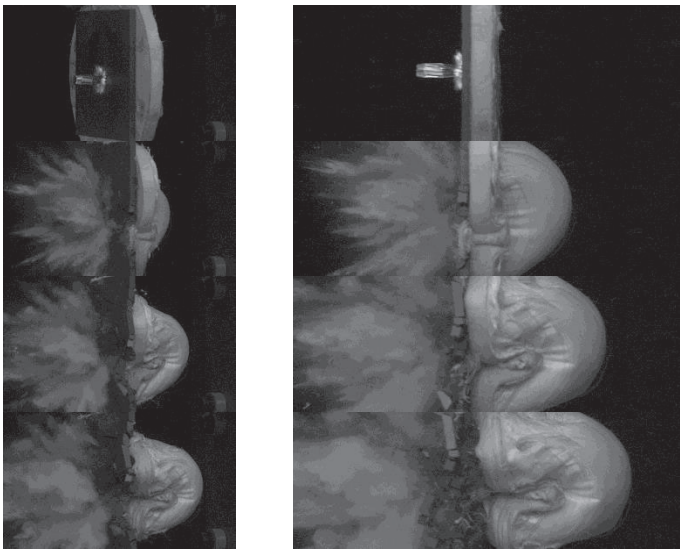

https://doi.org/10.52202/078352-0019

Figure 21. High-speed images of the final validation test. 232 µs interframe.

5 CONCLUSIONS

In conclusion, this paper has presented a characterization study for a ceramic and a composite material. The BBA approach has been established in order to use both numerical and experimental investigation.

Concerning the ceramic material, tests have been performed to identify model parameters. Numerical simulation was then used to provide complementary information and analyze the tests. EOS and HEL data of the material have been characterized and a good agreement with experiments is obtained from the simulation. However, the material damage process is complex, the study has enabled to clarify some part but there are still some questions remaining opened. Additional investigations are required towards the development of a ceramic ballistic predictive models. Overall, this project has been very enriching and will improve the way of studying the behavior of brittle materials under dynamic loading.

Concerning the UHMWPE composite, characterization tests have been conducted: in-plane tension, out-of-plane shear and compressive responses. UD fiber provides good tensile strength but the matrix low shear strength makes it prone to delamination, peeling and fiber slipping. The design of the tests has been driven by such specificity to acquire enough data to build the material model. The impact tests have highlighted the importance of ply slipping and temperature increase in the perforation mode. The simulation approach shows interesting results and the modelling scale choice represents a good compromise between calculation time and reproduction of main physical phenomena. This study should be pursued on a more detailed investigation of the failure mode of material at high temperature to confirm the modelling assumptions regarding fiber damage evolution.

At the end a final impact validation test on target made with a ceramic tile and a UHMWPE panel has been performed. This test still need to be compared with simulation results that are in progress.

Acknowledgments

The authors would like to thank the DGA Land Systems (French MoD) for financial support and all the team of Thiot Ingénierie laboratory for performing all the tests

References

[1] W. A. Gooch, "An overview of Ceramic Armor Applications," *Ceramic Transactions: Ceramic Armor Materials by Design,* vol. 134, pp. 3-22, 2001.

[2] C. E. Anderson, "A Review of Computational Ceramic Armor Modeling," *Advances in Ceramic Armor II: Ceramic Engineering and Science Proceedings,* vol. 27, pp. 1-18, 2006.

[3] H. Luo, W. Chen and A. M. Rajendran, "Dynamic Compressive Response of Damaged and Interlocked SiC-N Ceramics," *J. Am. Ceram. Soc,* vol. 89, pp. 266-273, 2005.

[4] R. Feng, G. F. Raiser and Y. M. Gupta, "Material strength and Inelastic Deformation of Silicon Carbide Under Shock Wave Compression," *J. Appl. Phys.,* vol. 83, pp. 79-86, 1997.

[5] G. R. Johnson and T. J. Holmquist, "Advances in Ceramic Armor: Ceramic Engineering and Science Proceedings," vol. 26, pp. 1-18, 2005.

[6] G. R. Johnson and T. J. Holmquist, "An improved computational constitutive model for brittle materials," *AIP Conf. Proc.,* vol. 309, p. 981, 1994.

[7] L. Govaert and P. J. Lenstra, *Cooloid Polym Sci. ,* vol. 270, 1992.

[8] P. J. Hazell, G. J. Appleby-Thomas, X. Trinquant and D. J. Chapman, *J. Applied Phys.,* vol. 110, 2011.

[9] J. P. Attwood, S. N. Khaderi, K. Karthikeyan, N. A. Fleck, M. R. O'Masta, H. N. G. Wadley and V. S. Deshpande, *J. Mech. Phy. Solids,* vol. 70, no. 200, 2014.

[10] T. Lassïg, F. Bagusat, M. May and S. Hiermaier, *Int. J. Impact Eng.,* vol. 86, no. 240, 2015.

[11] M. R. O'Masta, B. G. Compton, E. A. Gamble, F. W. Zok, V. S. Deshpande and H. N. G. Wadley, *Int. J. Impact Eng.,* vol. 86, no. 131, 2015.

[12] T. Lassïg, L. Nguyen, M. May, W. Riedel, U. Heisserer, H. V. D. Werf and S. Hiermaier, *Int. J. Impact Eng.,* vol. 75, no. 110, 2015.

[13] T. Dayyoub, A. V. Maksimkin, S. Kaloshkin, E. Kolesnikov, D. Chukov, T. P. Dyachkova and I. Gutnik, "The Structure and Mechanical Properties of the UHMWPE Films Modified by the Mixture of Graphene Nanoplates with Polyaniline," *Polymers,* vol. 11, no. 23, 2019.